

Gel point determination of gelatin hydrogels by dynamic light scattering and rheological measurements

Takuro Matsunaga and Mitsuhiro Shibayama*

Institute for Solid State Physics, The University of Tokyo, 5-1-5 Kashiwanoha, Kashiwa, 277-8581, Japan

(Received 7 May 2007; published 27 September 2007)

The sol-gel transition of gelatin aqueous solutions has been investigated in terms of time-resolved dynamic light scattering (DLS) and rheological measurements during the cooling process. A drastic increase in the scattering intensity, ergodic-nonergodic transition, and a power-law behavior in the scattering intensity-time correlation function were observed at the gelation temperature T_{gel} . Thus obtained “microscopic” T_{gel} was confirmed to be in good agreement with a “macroscopic” T_{gel} obtained by rheological measurements irrespective of gelatin concentration C . The fractal exponent D_p evaluated by DLS was found to be q and C independent and was also in good agreement with that obtained by rheology (n), i.e., $D_p \cong n \cong 0.73$, where q is the magnitude of the scattering vector.

DOI: [10.1103/PhysRevE.76.030401](https://doi.org/10.1103/PhysRevE.76.030401)

PACS number(s): 83.80.Kn, 46.35.+z, 78.35.+c

Sol-gel transition is a connectivity transition and the connectivity correlation diverges at the gel point. Classically, it was treated with a Bethe lattice [1] or a cascade problem [2]. Today, sol-gel transition is regarded as one of percolation phenomena [3,4]. A typical example is gelation of gelatin aqueous solutions [5]. Winter *et al.* found that the storage $G'(\omega)$ and loss moduli $G''(\omega)$ crossover and their ω dependencies become colinear at the gel point with $G'(\omega) \approx G''(\omega) \sim \omega^n$ [6,7]. Here, ω is the angular frequency and n is the viscoelastic exponent.

Martin *et al.* reported the critical dynamics of sol-gel transition during a process of chemical reaction of tetramethoxysilane (TMOS) in terms of dynamic light scattering (DLS) [8,9]. They demonstrated that the scattering intensity-time correlation function (ICF) $g^{(2)}(\tau)$ changed from a stretched exponential function to a power-law function, i.e., $g^{(2)}(\tau) - 1 \sim \tau^{-(1-D_p)}$ at a gel point. Here, D_p is “the fractal dimension of the detected photons” [8]. Ren and Sorensen investigated a similar behavior in thermoreversible gelatin gels [10,11]. Although similar values have been reported for n and D_p , e.g., $n \approx D_p \approx 0.73$ for gelatin, the relationship between n and D_p has been a controversial issue for more than a decade [12].

Sol-gel transition is also regarded as an ergodic-nonergodic transition [13]. The light scattering intensity becomes sample-position dependent at the gelation threshold and the contribution of frozen-concentration fluctuations to the scattering intensity becomes dominant [14,15]. It has been believed that scattering intensity does not diverge at the gel point as pointed out by de Gennes [16]. However, we observed that light scattering intensity exhibited a characteristic rise at the gel point in a chemical gelling system [15] and in thermoreversible physical gels as well, such as poly(vinyl alcohol) complex gels [17], gelatin [18,19], where the polymer concentration was always above the chain-overlap concentration. Hence, sol-gel transition is indeed an analogy of critical opalescence commonly observed in a vapor-liquid

transition. These findings led to recognition of one of the essential features of sol-gel transition, i.e., restriction of thermal concentration fluctuations by infinite connectivity [20], in other words, an ergodic-nonergodic transition. That is, an abrupt intensity rise in light scattering is a universal phenomenon originating from frozen-in concentration fluctuations, which give rise to light scattering that is much stronger than thermal concentration fluctuations.

On the basis of these findings, Shibayama *et al.* [21,22] proposed four methods of gel-point determination with dynamic light scattering (DLS). The gel point is determined as a point at which one of the following features is observed: (i) a drastic increase in the scattering intensity, (ii) a power-law behavior in ICF, (iii) a characteristic broadening in the distribution function obtained by inverse Laplace transform of ICF, or (iv) a depression of the initial amplitude of ICF. The applicability of these methods was confirmed for chemical gels, physical gels, gelators, and glass forming systems [23]. However, it has been an open question that this “microscopic” gel point is the same as the “macroscopic” gel point determined by rheological measurements. In this paper, we report on the equivalence of the gel points determined by DLS and rheological methods, and discuss the concentration and scattering angle dependence of the fractal exponents n and D_p .

The scattering ICF $g^{(2)}(\tau)$ between time t and $t+\tau$ is defined by

$$g^{(2)}(\tau) \equiv \frac{\langle I(t)I(t+\tau) \rangle_T}{\langle I(t) \rangle_T^2}, \quad (1)$$

where τ is the decay time and $\langle I(t) \rangle_T$ means time average scattering intensity. In a sol state, the ICF consists of a fast mode (a single exponential) and a slow mode (a stretched exponential function), as written by

$$g^{(2)}(\tau) - 1 = \sigma_1^2 \{ A \exp(-Dq^2\tau) + (1-A) \exp[-(\tau/\tau_c)^\beta] \}^2, \quad (2)$$

where σ_1^2 is the initial amplitude of ICF, D is the collective diffusion coefficient, A is the fraction of the fast mode, τ_c is

*<http://shibayama.issp.u-tokyo.ac.jp/mitsu/>; shibayama@issp.u-tokyo.ac.jp

the characteristic decay time for the slow mode, and β is the stretched exponent. When approaching a sol-gel transition point, the slow mode becomes dominant and ICF becomes a power-law function. Martin *et al.* proposed the following equation [Martin-Wilcoxon-Odinek (MWO) equation] [9], i.e.,

$$g^{(2)}(\tau) - 1 = \sigma_1^2 \left\{ A \exp(-Dq^2\tau) + \frac{(1-A)\exp(-\tau/\tau_{\max})}{[1+(\tau/\tau^*)]^{(1-D_p)/2}} \right\}^2 \sim \tau^{-(1-D_p)}. \quad (3)$$

Here, τ^* is the characteristic time where the power law behavior appears. Note that an exponential term with the large τ cutoff τ_{\max} is added in Eq. (3) [18]. According to Martin *et al.*, the fractal dimension of ICF is simply obtained as D_p since ICF is just a density-density correlation function of the detected photons per unit time and the time axis can be regarded as one-dimensional space.

Alkali-treated gelatin (type B; Lot No. P-3201, Nitta Gelatin Co., Osaka) was used without further purification. The molecular weight M_w was 1.45×10^5 Da and the isoelectric point was pH 4.97. Time-resolved DLS measurements were conducted with ALV5000 SLS/DLS goniometer, Langen, Germany. The light source was a 22 mW He-Ne laser (the wavelength $\lambda=632.8$ nm). The instrumental coherence factor was better than 0.95. Aqueous solutions of gelatin were dissolved in D_2O at 50°C , filtered with a $0.20 \mu\text{m}$ filter, and then cooled to 40°C . Series of ICFs were obtained for these gelatin solutions during the cooling process at a rate of $0.2^\circ\text{C}/\text{min}$. Delay of temperature response was less than 0.2°C . The sampling time for each ICF acquisition was 30 s each without intermission. Rheological experiments were also carried out on the same samples with MCR501, Anton Paar, Austria. Rheological properties, i.e., $G'(\omega)$ and $G''(\omega)$, were measured during the cooling process with a double-cylinder geometry with 26.7- and 28.9-mm-diameter cylinders. The strain γ and the angular frequency ω were 100% and 1.0 rad/s for the sol state ($40 \geq T \geq 30^\circ\text{C}$) respectively, and $\gamma=0.5\%$ and $\omega=1.0$ rad/s for the transition region and the gel state ($27 \geq T \geq 10^\circ\text{C}$). For ω dependent experiments, γ and T was chosen to be 20% and 16.0°C , respectively.

Figure 1(a) shows a series of ICFs for a 3.0 wt % gelatin aqueous solution in the cooling process. The scattering angle θ was 90° , corresponding to the magnitude of the scattering vector, $q=4\pi n_s \sin(\theta/2)/\lambda$, that was $1.87 \times 10^{-2} \text{ nm}^{-1}$, where n_s is the refractive index of the solvent. The ICF at the beginning, e.g., $t=5.1$ min ($T \approx 40^\circ\text{C}$), is well fitted with Eq. (2), indicating that the gelatin sol indeed has two modes, i.e., the fast mode (the so-called gel mode) and the slow mode. The fitted parameters are $D=1.31 \times 10^{-7} \text{ cm}^2/\text{s}$, $A=0.319$, $\tau_c=0.636$ ms, and $\beta=0.474$. The correlation length (or the mesh size) ξ can be estimated from D via $\xi=kT/6\pi\eta D$, where k is the Boltzmann constant, η is the solvent viscosity. ξ is obtained from D to be 2.67 nm. In addition, the slow mode is assigned to translational diffusion of finite gelatin clusters.

By cooling, finite gelatin clusters become larger and larger and the ICF accompanies a long tail at a slower relaxation time. At $t=85.2$ min ($T=25.3^\circ\text{C}$), the tail became the

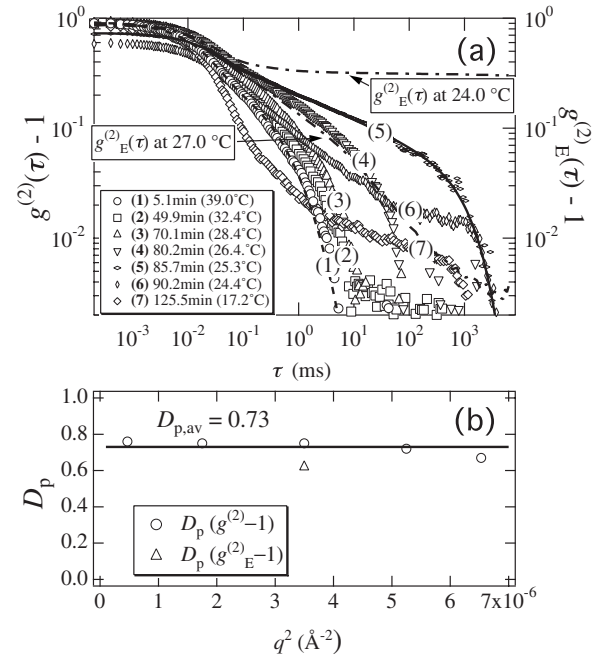


FIG. 1. (a) Left: Time-average ICFs of 3 wt %-gelatin aqueous solutions during gelation process at the scattering angle $\theta=90^\circ$. The dashed and solid lines are the curve fits with Eqs. (2) and (3), respectively. Right (chain line): Ensemble-average ICFs, $g_E^{(2)}(\tau)$, for before ($T=27.0^\circ\text{C}$) and after gel point ($T=24.0^\circ\text{C}$). (b) q dependence of D_p . The value near T_{gel} ($T=27.0^\circ\text{C}$) obtained by ensemble-average ICF is shown with a cross.

longest and the ICF was successfully fitted with Eq. (3) as shown with the solid line in the figure. The fitted parameters are $D=0.913 \times 10^{-7} \text{ cm}^2/\text{s}$, $A=0.189$, $\tau^*=0.013$ ms, $D_p=0.752$, and $\tau_{\max}=899$ ms. Since τ_{\max} is infinite, in principle, its finite value suggests an occurrence of volume-filling before formation of infinite clusters. The value of D_p was independent of the sample position. Figure 1(a) shows the ensemble average ICF [13],

$$g_E^{(2)}(\tau) = \frac{(1/N) \sum_j \langle I_{T,j}^2 g_j^{(2)}(\tau) \rangle}{\left\{ (1/N) \sum_j \langle I_{T,j} \rangle \right\}^2}, \quad (4)$$

obtained at different sample positions j [$1 \leq j \leq N(=100)$], before ($T=27.0^\circ\text{C}$) and after gel point ($T=24.0^\circ\text{C}$). The curve at $T=27.0^\circ\text{C}$ shows that $g_E^{(2)}(\tau)$ is also represented by a power-law function at a gel point. However, an accurate determination with $g_E^{(2)}(\tau)$ is experimentally difficult for the gelling system because of (1) the necessity of sampling at many data points without quenching the gelation process and (2) the domination of the frozen component after the gel point as shown in the curve at $T=24.0^\circ\text{C}$. Hence, it is preferable to use time-average ICF for gel-point determination. Figure 1(b) shows the variation of the fractal exponents D_p 's evaluated with Eq. (3). The triangle denotes that obtained from $g_E^{(2)}(\tau)$. Because the temperature was not the same as

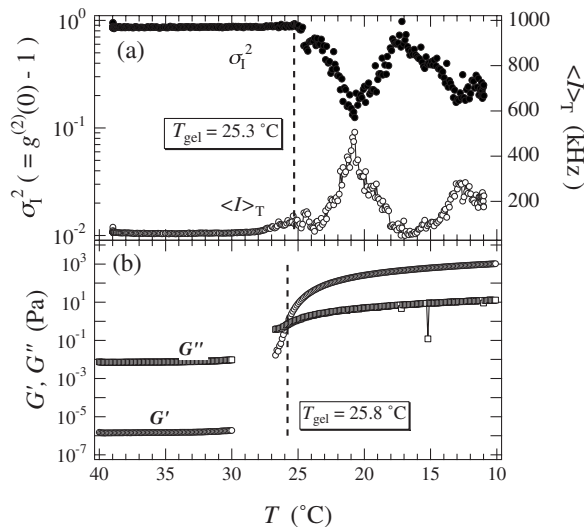


FIG. 2. Variations of scattering and rheological properties of 3.0% gelatin aqueous solution. (a) The scattering intensity $\langle I \rangle_T$ and the initial amplitude of ICF σ_1^2 , (b) the storage G' and loss moduli G'' . The cooling rate was $0.2 \text{ }^\circ\text{C}/\text{min}$.

T_{gel} , this value is somewhat lower than those obtained by the time-average ICF. The observed values of D_p seem to be q independent, unlike the results reported by Ren and Sorensen [10,11]. Since this exponent is related to the rheological exponent ($q \rightarrow 0$) at the sol-gel transition, it should be size independent and hence q independent. As a matter of fact, the value of the exponent $D_p = 0.752$ is in good agreement with that reported for gelatin hydrogels ($D_p = 0.74$) [18] and for TMOS ($D_p = 0.73$) [9]. Note that a much smaller value of D_p (≈ 0.4) was obtained in gelatin gels when the polymer concentration was close to the chain-overlap concentration ($C \approx 0.3 \text{ wt } \%$) [19]. In this case, hydrodynamic interaction is not screened, giving a different value of n as predicted by Muthukumar for the rheological fractal exponent [24]. Ikkai reported $D_p \approx 0.4$ for poly(vinyl alcohol) Congo Red thermoreversible hydrogels [17], where electrostatic interaction may play a significant role. Hence, the value of D_p itself seems to be dependent on the kind of gels.

Now let us compare the results of the sol-gel transition temperatures obtained by DLS and by rheological measurements. As introduced above, a gel point can be determined where the light scattering intensity increases drastically. Figure 2(a) shows the variations of the time-average scattering intensity $\langle I \rangle_T$ at the scattering angle $\theta = 90^\circ$, and σ_1^2 . Note that this point, $T_{\text{gel}} = 25.3 \text{ }^\circ\text{C}$, is the same as that determined from ICF (see, Fig. 1). The gel point is more clearly observed as a deviation of σ_1^2 from unity. This is due to ergodic-nonergodic transition [13]. That is, the time-independent frozen component in $\langle I \rangle_T$ becomes significantly larger than the dynamic component. Hence, the gel point can be uniquely determined by DLS. On the other hand, Fig. 2(b) shows the variations of G' and G'' as functions of cooling temperature. A T_{gel} was determined to be $25.8 \text{ }^\circ\text{C}$ at $G' = G''$. As demonstrated in the figure, T_{gel} obtained by the rheological method agrees well with that obtained by DLS within $\pm 1.0 \text{ }^\circ\text{C}$. It should be emphasized that this confirms the equivalence of the gel points

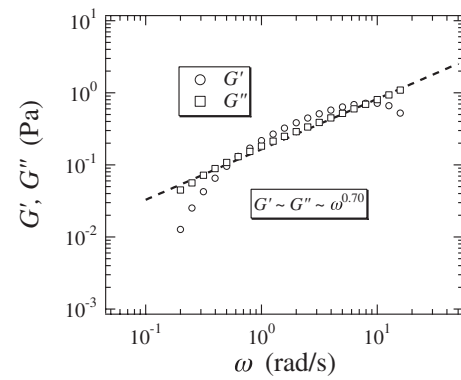


FIG. 3. Angular frequency dependence of the storage $G'(\omega)$ and the loss moduli $G''(\omega)$ for 1 wt % gelatin aqueous solution near the gel point (at $16.0 \text{ }^\circ\text{C}$).

obtained by microscopic DLS measurements and by macroscopic rheological measurements. By definition, connectivity diverges at a gel point, meaning that the whole system is percolated. DLS, on the other hand, the irradiating volume is very small in the sample, e.g., order of $1 \times 10^{-3} \text{ mm}^3$. Hence, a critique such that the dynamics in such a small volume may be different from that in the whole sample, has often been raised. The experimental finding disclosed in this work indicates that connectivity transition can be observed irrespective of the system size although there is a lower bound. Small-angle neutron scattering (SANS) on the same system showed only a slight increase in the scattering intensity at low q region ($\leq 0.2 \text{ nm}^{-1}$) (not shown here). This means that SANS is not sensitive to gel point determination of physical gels. On the other hand, the q range of light scattering (including DLS) is small enough to detect a gel point and is a suitable measure to determine gel points.

Figure 3 shows plots of $G'(\omega)$ and $G''(\omega)$ for 1 wt % gelatin solution near the gel point $T_{\text{gel}} (\approx 16.0 \text{ }^\circ\text{C})$. The data are colinear with respect to ω with $n = 0.70 \pm 0.02$. This observation together with the DLS results eloquently suggests that the physical meaning of D_p and n is the same and the value is around 0.73 at least for gelatin hydrogels. Note that it came to our attention that the value of n reported by Peyrelasse *et al.* for a gelatin system was 0.62 [25]. The difference may be partially ascribed to the difference in the molecular weight of gelatin ($M_w = 2.95 \times 10^3 \text{ Da}$) and in the chemical structure.

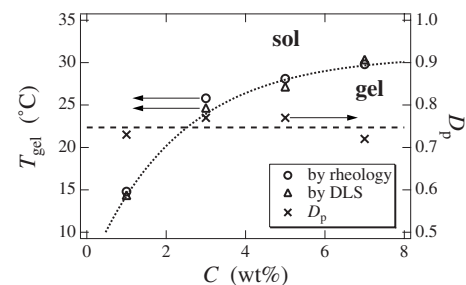


FIG. 4. Sol-gel phase diagram for gelatin aqueous systems. C dependence of T_{gel} and D_p .

Figure 4 shows the concentration dependencies of the sol-gel transition temperatures and the exponent D_p . These temperatures were obtained with the method discussed in Fig. 2. As shown in the figure, T_{gel} increases as increasing C . This type of sol-gel phase diagram is exactly the same as that predicted by site-bond percolation theory [27]. The T_{gel} s obtained by DLS and the rheological measurement agree well within the experimental error of less than 1.0 °C. Hence, it is concluded that both DLS and rheological measurements provide essentially the same T_{gel} in a wide range of C and q . More interestingly, the fractal exponent D_p is C independent and is the same as n for the gelatin systems investigated in this work and its value is about 0.73. Note that Richter *et al.* also reported an equality between n and D_p , i.e., $n=D_p=0.59$ for thermoreversible gels of xanthan gum and locust bean gum [26].

The sol-gel transition temperature T_{gel} was determined for

gelatin aqueous solutions by DLS and rheological measurements. An abrupt increase in light scattering intensity, a power-law behavior in ICF, suppression of σ_1^2 , and a crossover in $G'(\omega)$ and $G''(\omega)$ were observed at the same temperature, i.e., T_{gel} . We obtain an agreement of T_{gel} obtained microscopic light scattering and macroscopic rheological measurements in a wide range of polymer concentrations C . The fractal exponent D_p was found to be q and C independent and is the same as that obtained by rheological measurements n , indicating that D_p is a parameter describing the architecture of gels.

This work was partially supported by the Ministry of Education, Science, Sports and Culture, Japan [Grant-in-Aid for Scientific Research (A), 2006–2008, No. 18205025, and for Scientific Research on Priority Areas, 2006-2010, No. 18068004].

-
- [1] W. H. Stockmayer, *J. Chem. Phys.* **11**, 45 (1943).
 [2] G. R. Dobson and M. Gordon, *J. Chem. Phys.* **43**, 705 (1965).
 [3] D. Stauffer, *J. Chem. Soc., Faraday Trans. 2* **72**, 1354 (1976).
 [4] D. Stauffer, *Introduction to Percolation Theory* (Taylor & Francis, London, 1985).
 [5] J. M. Guenet, *Thermoreversible Gelation of Polymers and Biopolymers* (Academic, New York, 1992).
 [6] H. H. Winter, P. J. Morganelli, and F. Chambon, *J. Rheol.* **30**, 367 (1986).
 [7] H. H. Winter and M. Mours, *Adv. Polym. Sci.* **134**, 167 (1997).
 [8] J. E. Martin and J. P. Wilcoxon, *Phys. Rev. Lett.* **61**, 373 (1988).
 [9] J. E. Martin, J. Wilcoxon, and J. Odinek, *Phys. Rev. A* **43**, 858 (1991).
 [10] S. Z. Ren, W. F. Shi, W. B. Zhang, and C. M. Sorensen, *Phys. Rev. A* **45**, 2416 (1992).
 [11] S. Z. Ren and C. M. Sorensen, *Phys. Rev. Lett.* **70**, 1727 (1993).
 [12] M. Adam and D. Lairez, in *The Physical Properties of Polymeric Gels*, edited by J. P. Cohen Addad (Wiley, New York, 1996).
 [13] P. N. Pusey and W. van Megen, *Physica A* **157**, 705 (1989).
 [14] J. G. H. Joosten, J. L. McCarthy, and P. N. Pusey, *Macromolecules* **25**, 6690 (1991).
 [15] T. Norisuye, M. Shibayama, and S. Nomura, *Polymer* **39**, 2769 (1998).
 [16] P. G. de Gennes, *J. Phys. (France) Lett.* **40**, 197 (1979).
 [17] F. Ikkai and M. Shibayama, *Phys. Rev. Lett.* **82**, 4946 (1999).
 [18] M. Okamoto, T. Norisuye, and M. Shibayama, *Macromolecules* **34**, 8496 (2001).
 [19] M. Shibayama and M. Okamoto, *J. Chem. Phys.* **115**, 4285 (2001).
 [20] S. Panyukov and Y. Rabin, *Phys. Rep.* **269**, 1 (1996).
 [21] M. Shibayama, S. Takata, and T. Norisuye, *Physica A* **249**, 245 (1998).
 [22] M. Shibayama and T. Norisuye, *Bull. Chem. Soc. Jpn.* **75**, 641 (2002).
 [23] M. Shibayama, *Bull. Chem. Soc. Jpn.* **79**, 1799 (2006).
 [24] M. Muthukumar, *Macromolecules* **22**, 4658 (1989).
 [25] J. Peyrelasse, M. Lamarque, J. P. Habas, and N. El Bounia, *Phys. Rev. E* **53**, 6126 (1996).
 [26] S. Richter, R. Matzker, and K. Schröter, *Macromol. Rapid Commun.* **26**, 1626 (2005).
 [27] A. Coniglio, H. E. Stanley, and W. Klein, *Phys. Rev. Lett.* **42**, 518 (1979).